NAVAL POSTGRADUATE SCHOOL

MONTEREY, CALIFORNIA

THESIS

INVESTIGATION OF OUTER LENGTH SCALE IN OPTICAL TURBULENCE

by

Steven S.M. Lim

December 2003

Thesis Advisor: D.L. Walters
Co-Advisor: D.K. Miller

THIS PAGE INTENTIONALLY LEFT BLANK

REPORT DOCUMENTATION PAGE		Form Approved OMB No. 0704-0188

1. AGENCY USE ONLY *(Leave blank)*	2. REPORT DATE December 2003	3. REPORT TYPE AND DATES COVERED Master's Thesis

4. TITLE AND SUBTITLE: Investigation of Outer Length Scale In Optical Turbulence	5. FUNDING NUMBERS
6. AUTHOR(S) CPT Steven S.M. Lim	
7. PERFORMING ORGANIZATION NAME(S) AND ADDRESS(ES) Naval Postgraduate School Monterey, CA 93943-5000	8. PERFORMING ORGANIZATION REPORT NUMBER
9. SPONSORING /MONITORING AGENCY NAME(S) AND ADDRESS(ES) N/A	10. SPONSORING/MONITORING AGENCY REPORT NUMBER

11. SUPPLEMENTARY NOTES The views expressed in this thesis are those of the author and do not reflect the official policy or position of the Department of Defense or the U.S. Government.

12a. DISTRIBUTION / AVAILABILITY STATEMENT Approved for Public Release,Distribution is Unlimited	12b. DISTRIBUTION CODE

13. ABSTRACT (maximum 200 words)

Atmospheric turbulence degrades the electromagnetic propagation medium and affects many military applications. The strength and spatial distribution of turbulence are critical parameters that arise in theoretical modeling and experimental situations. This thesis investigated three outer scales of turbulence using experimental data from two instruments: microthermal probes carried by a balloon and an acoustic sounder. The outer length scale is the size of the largest energy-containing eddy in a turbulent region of the atmosphere. The length scales considered were the thermal length scale l_h associated with temperature fluctuations, the momentum length scale l_m, which represents the size of the velocity fluctuations and the boundary thermal convective cell size. The microthermal balloon data had excessive scatter when the thermal outer scale was expressed in terms of the gradient Richardson number. A reasonable functional relationship was not found and unrealistic outer scales l_h > 1000m and Ri_g > 100 prevailed. The primary reason was that inadequate sampling of the turbulent layers prevented the computation of valid statistical averages. The volume backscatter cross-section measured by an acoustic sounder provided better statistical averaging of the optical structure parameter C_n^2 than the microthermal balloon data. The separation of daytime convective thermal plumes was found from the acoustic sounder data by computing average C_n^2 values between 20 to 50 meters for each acoustic pulse and performing an autocorrelation of these averages over 600 seconds. Multiplying the autocorrelation time by the wind speed gave the separation between the convective thermal maxima and their minima. The mean correlation length for March 2002 at the Starfire Optical Range was 1590 $\pm$ 770 meters, between 1000 and 1600 local time. This length is proportional to the convective thermal cell size and to the boundary layer inversion height. A smaller length scale of 200 meters also appeared in the acoustic sounder data associated with the local height of the data and the hill above the ground.

14. SUBJECT TERMS Atmospheric Structure Parameter, Atmospheric turbulence, Outer Length Scale, Richardson Number, Acoustic Sounder, Thermosonde, Optical turbulence	15. NUMBER OF PAGES 53
	16. PRICE CODE

17. SECURITY CLASSIFICATION OF REPORT	18. SECURITY CLASSIFICATION OF THIS PAGE	19. SECURITY CLASSIFICATION OF ABSTRACT	20. LIMITATION OF ABSTRACT
Unclassified	Unclassified	Unclassified	UL

NSN 7540-01-280-5500

Standard Form 298 (Rev. 2-89)
Prescribed by ANSI Std. 239-18

THIS PAGE INTENTIONALLY LEFT BLANK

Approved for public release; distribution is unlimited

INVESTIGATION OF OUTER LENGTH SCALE IN OPTICAL TURBULENCE

Steven S.M. Lim
Captain, Republic of Singapore Army
B. Engrg (Mech), Nanyang Technological University, 1998

Submitted in partial fulfillment of the
requirements for the degree of

MASTER OF SCIENCE IN COMBAT SYSTEMS TECHNOLOGY

from the

NAVAL POSTGRADUATE SCHOOL
December 2003

Author: Steven S.M. Lim

Approved by: D.L. Walters
Thesis Advisor

D.K. Miller
Co-Advisor

J. H. Luscombe
Chairman, Department of Physics

THIS PAGE INTENTIONALLY LEFT BLANK

ABSTRACT

Atmospheric turbulence degrades the electromagnetic propagation medium and affects many military applications. The strength and spatial distribution of turbulence are critical parameters that arise in theoretical modeling and experimental situations. This thesis investigated three outer scales of turbulence using experimental data from two instruments: microthermal probes carried by a balloon and an acoustic sounder. The outer length scale is the size of the largest energy-containing eddy in a turbulent region of the atmosphere. The length scales considered were the thermal length scale l_h associated with temperature fluctuations, the momentum length scale l_m, which represents the size of the velocity fluctuations and the boundary thermal convective cell size. The microthermal balloon data had excessive scatter when the thermal outer scale was expressed in terms of the gradient Richardson number. A reasonable functional relationship was not found and unrealistic outer scales l_h > 1000m and Ri_g > 100 prevailed. The primary reason was that inadequate sampling of the turbulent layers prevented the computation of valid statistical averages. The volume backscatter cross-section measured by an acoustic sounder provided better statistical averaging of the optical structure parameter C_n^2 than the microthermal balloon data. The separation of daytime convective thermal plumes was found from the acoustic sounder data by computing average C_n^2 values between 20 to 50 meters for each acoustic pulse and performing an autocorrelation of these averages over 600 seconds. Multiplying the autocorrelation time by the wind speed gave the separation between the convective thermal maxima and their minima. The mean correlation length for March 2002 at the Starfire Optical Range was 1590 $\pm$ 770 meters, between 1000 and 1600 local time. This length is proportional to the convective thermal cell size and to the boundary layer inversion height. A smaller length scale of 200 meters also appeared in the acoustic sounder data associated with the local height of the data and the hill above the ground.

THIS PAGE INTENTIONALLY LEFT BLANK

TABLE OF CONTENTS

THIS PAGE INTENTIONALLY LEFT BLANK

LIST OF FIGURES

THIS PAGE INTENTIONALLY LEFT BLANK

LIST OF TABLES

THIS PAGE INTENTIONALLY LEFT BLANK

ACKNOWLEDGMENTS

I would like to express my sincere appreciation and gratitude to Professor Walters for his overwhelming support and guidance throughout the process of this thesis. He was always available and willing to work at all hours to ensure this project was a success.

Above all, I would like to express my deepest thanks to my loving and devoted wife, Josephine. She is a loving and dedicated mother to our son Ryan. Her patience, understanding, and remarkable ability to maintain a pleasant, comforting home during this highly stressful time made this process possible. Thank you Lord, Your grace is always sufficient in my weakness.

THIS PAGE INTENTIONALLY LEFT BLANK

I. INTRODUCTION

A. OBJECTIVES

Atmospheric turbulence is an important area of study in the propagation of electromagnetic waves because it degrades the propagation medium. Fluctuations in atmospheric pressure and temperature cause fluctuations in the air's index of refraction, i.e. optical turbulence, which in turn distort the phases of propagating waves. Optical turbulence is produced by two mechanisms: Near the surface, the heat flux interchange between the earth's surface and the air is the dominant contributor. Above the surface, mixing of air with different temperatures by vertical wind shear is the dominant mechanism.

Besides degrading imaging systems, optical turbulence also causes beam wander and spreading in laser applications. The understanding of atmospheric turbulence and its effects is critical to some military systems. With the growing use of lasers in laser guided bombs, laser designation and ranging devices in the military, it has become a necessity to understand the degrading effects of atmospheric turbulence on these systems.

Different parameters characterize optical turbulence. One of the most important is the optical structure parameter C_n^2, which contributes to most other variables such as the coherence length r_o, isoplanatic angle θ_{AO}, and Greenwood frequency f_g (Sasiela 1994). The parameter C_n^2 is valid over a range of scale sizes extending from an inner scale on the order of one centimeter to an outer scale L_0 of meters, known as the inertial range. The outer scale size is of particular interest since it reflects the physical boundary conditions involved in the generation of turbulence and is a critical scale needed for turbulence modeling. This thesis focused on three different outer scale lengths, the thermal turbulence length scale l_h, the turbulent velocity length scale l_m, and a horizontal convective scale L_c.

The objective of this thesis was to estimate the outer length scales using data from two instruments: micro-thermal probes and an acoustic sounder. Using the first data source, the purpose was to examine the relationship between the length scales l_h and l_m at different altitudes and the gradient Richardson number Ri_g using experimental data from balloon launches. The data used for this study was a series of 27 micro-thermal balloon launches taken by the U.S. Air Force Research Laboratory (AFRL) from 27 February through 8 March 2002 at Vandenberg Air Force Base located in southwest coastal California. The Air Force conducted three micro-thermal launches a night starting just after sunset and each launch was two hours apart. Data was collected during the night because of the daytime solar heating of the temperature probes, which produced erroneous data during day launches (Richardson 1997). The thermosondes measured root mean square (RMS) temperature differences with a pair of 3.8-micron fast response temperature probes attached to a balloon launch device (Brown *et al.* 1982).

Using the second data source, the size of the convective boundary layer scale L_c was explored using acoustic data. An acoustic sounder was directed vertically into the atmosphere to collect turbulent atmospheric data from 1 March to 29 March 2002 at the Starfire Optical Range in Kirtland Air Force Base, New Mexico.

B. BACKGROUND

1. Modeling Turbulence with Length Scales

Length scales play an important role in understanding atmospheric turbulence. Similar to the characteristic length in the Reynolds number, which sets the conditions for turbulent and laminar flow, the length scale is a scale size of the energy source. In addition, the length scale helps resolve the closure problem in turbulence modeling.

Turbulence is a random and non-linear phenomenon and many attempts have been made to model the process. The Navier Stokes equations describe atmospheric turbulence but the enormous computational problem restricts solutions to small Reynolds numbers (~10^3 – 10^4). Reynolds' decomposition of a flow variable into a mean quantity, e.g. $\bar{U}$ and a fluctuating component, e.g. u' helps to simplify the problem but introduces new variables, creating the closure problem (Beland 1996).

To handle the closure problem presented by the cross-correlation fluxes such as $\langle u'w' \rangle$, $\langle v'w' \rangle$, and $\langle \theta'w' \rangle$, turbulence parameterization schemes represent turbulent fluxes in terms of the bulk meteorological variables pressure, temperature, wind speed and their gradients. First order closure parameterizations approximate the turbulent momentum and heat fluxes as gradients

$$\langle u'w' \rangle = -K_m \frac{\partial \bar{U}}{\partial z}, \quad \langle v'w' \rangle = -K_m \frac{\partial \bar{V}}{\partial z}, \quad \langle w'\theta' \rangle = -K_h \frac{\partial \bar{\theta}}{\partial z} \quad , \tag{1}$$

where K_m and K_h are the exchange coefficients for momentum and heat. The K parameters relate the fluxes to gradients in the mean wind and temperature fields and are analogous to diffusion coefficients in the kinetic theory of gas. There are many models that describe the K-parameters and the use of turbulence parameterization shifts the closure problem to one prescribing the correct K parameters (Sorbjan 1989). While first order closure model treats the K parameters as constants, higher order models express K parameters as functions of a length or time scale, or the Richardson number (to be discussed later). The characteristic length scale, also called the mixing length turns out to be a key parameter of these models and largely governs the accuracy of the predicted turbulence (Andrén 1990).

However, determining the proper length scale is difficult since it varies from tens to hundreds of meters and the mixing processes between heat and momentum are quite different (Koracin and Rogers 1990). Although an

assumption was often made about the existence of a “master length scale” to which all other closure length scales are related, the formulation of the master length scale is often done by trial and error and only applies to a specific region like the boundary layer. Instead of using experimental data, most length scales are formulated to achieve a preferred model behavior (Tjernström 1993). Experimental data has proven useful in determining length scale patterns in the atmospheric boundary layer (ABL), which has a depth of 1-2 km above sea level. However, data needed to determine the scale above the ABL is usually insufficient, making parameterization difficult.

Within a turbulent region there are different length scales. The thermal length scale, l_h, is associated with temperature fluctuations and the momentum length scale, l_m, represents the size of velocity fluctuations. During the day, heating of the earth’s surface by the sun forms thermal convective cells of horizontal size L_c within the boundary layer. This research focuses on 2 different data sources in investigating the length scales: micro-thermal balloon data and data from acoustic sounder measurements.

2. Thermosonde Measurement

The purpose of the first investigation was to examine the relationship between the thermal length scale l_h and the gradient Richardson number Ri_g using experimental data from balloon launches. Several atmospheric parameters influence the thermal length scale and the gradient Richardson number Ri_g and it is necessary to explain how these parameters affect one another.

a. Kolmogorov's Approach to Turbulence

To deal with the randomness of atmospheric turbulence, Kolmogorov used a statistical approach that relies on dimensional analysis to handle the spatial and temporal fluctuations (Max 2003). By assuming homogeneity and isotropy at least in a local volume, and if the random processes have slowing varying means, structure functions represent the intensity of the fluctuations of $f(r_1,r_2)$ over a distance between r_1 and r_2. Using the mean square differences, the structure function of $f(r_1,r_2)$ is:

$$D_f(\vec{r_1},\vec{r_2}) = \left\langle \left[f(\vec{r_1}) - f(\vec{r_2}) \right]^2 \right\rangle. \tag{2}$$

According to Kolmogorov's turbulence theory, turbulent eddies range in size from macroscale to microscale, forming a continuum of decreasing eddy sizes. Energy from convection and wind shear is first added to the system at the outer scale L_0 (10's - 100's of meters) before it cascades to a smaller scale l_0 (~ 1cm) where viscosity converts the energy to heat (Andrews 2001). By dimensional arguments and assuming an incompressible isotropic, homogeneous medium, Kolmogorov showed that the longitudinal structure function of the velocity is:

$$D_v(r) = C_v^2 r^{2/3}, \qquad l_0 < r < L_0. \tag{3}$$

The $r^{2/3}$ proportionality of the structure function in the inertial range ($l_0 < r < L_0$) applies to other structure functions such as temperature and refractive index. The refractive index structure function is:

$$D_n(r) = C_n^2 r^{2/3}, \tag{4}$$

where C_n^2 is the refractive index structure parameter, or the optical turbulence parameter ($m^{-2/3}$). Comparing equations (2) and (4), the refractive index structure parameter has the form:

$$C_n^2 = \frac{\left\langle (n_1 - n_2)^2 \right\rangle}{r^{2/3}}. \tag{5}$$

While C_n^2 is the critical parameter that describes optical turbulence, it is extremely difficult to measure C_n^2 directly using standard techniques since the index of refraction of the atmosphere is influenced by the atmosphere's temperature, pressure, moisture and the wavelength of the electromagnetic wave. However, C_n^2 depends on the temperature structure parameter, C_T^2 which can be measured directly. C_T^2 has a mathematical form similar to C_n^2:

$$C_T^2 = \frac{\left\langle (T_1 - T_2)^2 \right\rangle}{r^{2/3}}. \tag{6}$$

Though the refractive index depends on the dry-air wavelength, it is typical to ignore the wavelength dependence and assume a wavelength of 0.5μm (Beland 1996). The index of refraction is

$$n = 1 + 79 \times 10^{-6} P / T \,. \tag{7}$$

Taking the partial derivative of the air density with respect to the temperature and assuming isobaric density fluctuations, the optical turbulence parameter C_n^2 relates to the temperature structure parameter C_T^2 by

$$C_n^2 = \left(\frac{\partial n}{\partial T} \right)^2 C_T^2 = \left(79 \times 10^{-6} \frac{P}{T^2} \right)^2 C_T^2, \tag{8}$$

where C_n^2 is the optical turbulence parameter in $m^{-2/3}$, C_T^2 is the temperature structure parameter in $K^2 m^{-2/3} Pa^{-2}$, P is the air pressure in mbar and T is the air temperature in Kelvin. Therefore, the temperature structure parameter C_T^2 is

$$C_T^2 = \frac{C_n^2}{\left(79 \times 10^{-6} \frac{P}{T^2} \right)^2}. \tag{9}$$

b. The Outer Length Scale

In meteorology, the potential temperature θ for dry airflow is a conserved property. It is the temperature of a dry parcel of air at temperature T and pressure P transported adiabatically to a reference pressure P_{ref}, typically set at 1000 mb. Mathematically, the potential temperature, θ is

$$\theta = T\left(\frac{P_{ref}}{P}\right)^{\frac{R}{C_p}}, \tag{10}$$

where R is the universal gas constant and C_p is the specific heat capacity at constant pressure.

Both C_n^2 and C_T^2 vary with height and location. To account for these variations, Tatarskii (1961) related the altitude dependent temperature structure parameter $C_T^2(z)$ to an outer scale L_0 by

$$C_T^2(z) = aL_o^{4/3}(z)\left(\frac{d\theta}{dz}\frac{T(z)}{\theta(z)}\right)^2. \tag{11}$$

where L_0 is a length scale in meters, θ is the potential temperature in Kelvin and a ~ 2.8. The outer scale L_0 in equation (11) does not distinguish between the thermal l_h and velocity l_m length scales. The distinction between the two has evolved in more recent experimental work within the last decade. Since equation (11) relates the temperature structure parameter to the potential temperature gradient, the length scale L_0 is actually a thermal length scale l_h.

The objective of the first part of this thesis was to use the microthermal balloon data and equation (11) to solve for the thermal length scale l_h. Equating equations (9) and (11)

$$l_h = \left[\frac{C_n^2}{a} \left(\frac{79 \times 10^{-6} P}{T\theta} \frac{d\theta}{dz} \right)^{-2} \right]^{3/4} . \quad (12)$$

The difference in potential temperature at two different locations from equation (10) is

$$\theta_2 - \theta_1 = \left(\frac{P_{ref}}{P_1} \right)^{R/C_p} \left(T_2 \left(\frac{P_1}{P_2} \right)^{R/C_p} - T_1 \right). \quad (13)$$

The reference pressure introduces an artifact in the potential temperature difference $\left(\frac{P_{ref}}{P_1} \right)^{R/Cp}$ because mixing does not extend all the way to the surface. When computing C_T^2, the adiabatic temperature change induced by turbulence is the second term

$$\left(T_2 \left(\frac{P_1}{P_2} \right)^{R/C_p} - T_1 \right), \quad (14)$$

which requires using a local pressure reference $P_{ref} = P_1$. Therefore the local potential temperature gradient is

$$\left(\frac{d\theta}{dz} \right)_{local} = \frac{\theta_2 - \theta_1}{z_2 - z_1} = \frac{\left(T_2 \left(\frac{P_1}{P_2} \right)^{R/C_p} - T_1 \right)}{z_2 - z_1}. \quad (15)$$

Equivalently, using equations (10) and (13), another form for the equation is

$$\left(\frac{d\theta}{dz} \right)_{local} = \frac{d\theta}{dz} \frac{T(z)}{\theta(z)}. \quad (16)$$

Using equations (12), (15) and (16), the thermal length scale, l_h becomes

$$I_h = \left[\frac{\overline{C_n^2}(z_1, z_2)}{a\left(79\times10^{-6}\,\frac{P_1}{T_1^2}\right)^2} \left(\frac{T_2\left(\frac{P_1}{P_2}\right)^{R/C_p} - T_1}{z_2 - z_1} \right)^{-2} \right]^{3/4}, \qquad (17)$$

where $\overline{C_n^2}(z_1, z_2)$ is the average C_n^2 between z_1 and z_2.

c. Gradient Richardson Number, Ri_g

Atmospheric turbulence can also be described by the gradient Richardson number, Ri_g which relates the buoyant production of turbulence over the shear production of turbulence, i.e. free to forced convection. The gradient Richardson number is:

$$Ri_g = \frac{\frac{g}{\theta}\left(\frac{d\theta}{dz}\right)}{\left(\frac{dU}{dz}\right)^2 + \left(\frac{dV}{dz}\right)^2}, \qquad (18)$$

where U is magnitude of wind in the East direction, V is the magnitude of wind in the North direction and g is the gravitational constant, 9.81 m/s^2.

Substituting equations (15) and (16) into (18), the gradient Richardson number is:

$$Ri_g = \frac{\frac{g}{\theta_1}\left(\frac{\theta_2 - \theta_1}{z_2 - z_2}\right)}{\left(\frac{U_2 - U_1}{z_2 - z_2}\right)^2 + \left(\frac{V_2 - V_1}{z_2 - z_2}\right)^2}. \qquad (19)$$

When buoyancy forces displace the atmospheric flow vertically, they form hydro-dynamical unstable zones, leading to turbulence (Vernin and Avila 1998). Thus the gradient Richardson number gives an indication when turbulent motions will occur. Turbulent velocity fluctuations mix the air inducing

optical turbulence and C_T^2. Table 1 below shows the relationship between the gradient Richardson number and turbulence.

Potential Temperature Gradient ($\partial\theta/\partial z$)	**Static Stability**	**Ri_g**	**Flow**
> 0	Stable	> ¼	Laminar
> 0	Stable	0< Ri_g < ¼	Turbulent
0	Neutral	0	Turbulent
< 0	Unstable	< 0	Convective (Turbulent)

Table 1. Values of the gradient Richardson number for different types of flows (After Vernin and Avila 1998)

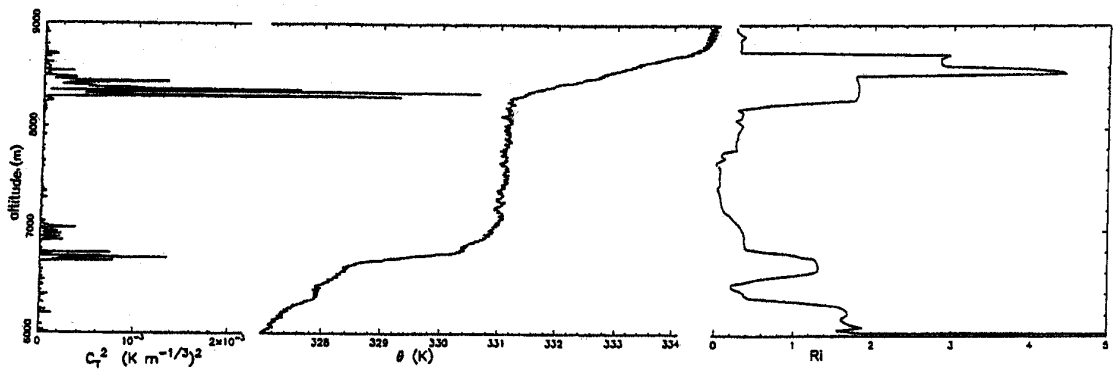

Figure 1. Profiles of the temperature structure parameter C_T^2, the potential temperature θ and the gradient Richardson number Ri_g (From Vernin and Avila 1998).

Figure 1 compares the experimental microthermal balloon measurements of the temperature structure parameter $C_T^2(z)$ to the potential temperature θ and the gradient Richardson number Ri_g. Strong C_T^2 layers appear at 6800 and 8400 meters at the upper and lower boundaries of the turbulent mixed region seen in the middle plot between 7000 and 8200 meters. This region has a potential temperature gradient near zero with a small

Richardson number, which requires forceful, turbulent mixing to create and maintain.

The vertical extent of the region of strong $C_T^2(z)$ seen in Figure 1 is a measure of the thermal length scale l_h seen in equations (11) and (12). The full width half maximum of the intense C_T^2 patches is around 100-200 meters. The middle plot shows that the turbulent velocity length scale l_m, where the potential temperature is nearly constant, was about 1000m. The gradient Richardson number Ri_g drops throughout this constant potential temperature region. Tjernström conducted an analysis of meteorological measurements collected by an aircraft to relate the l_h and l_m length scales, to the gradient Richardson number (Tjernström 1993).

d. Tjernström's Analysis

In 1989, Tjernström conducted a series of aircraft measurements to analyze different turbulent length scales in terms of the gradient Richardson number (Tjernström 1993). He collected turbulence data at 50 Hz between 30 and 2000 m above the ocean off the southeast Baltic coast of Sweden. He measured the length of turbulent temperature sequences of data collected during shallow descents through turbulent layers of the atmosphere. He found a good relationship between the thermal length scale l_h and the gradient Richardson number, as seen in Figure 2, and a similar relationship for the ratio of the exchange coefficients K_m to K_h of equation (1).

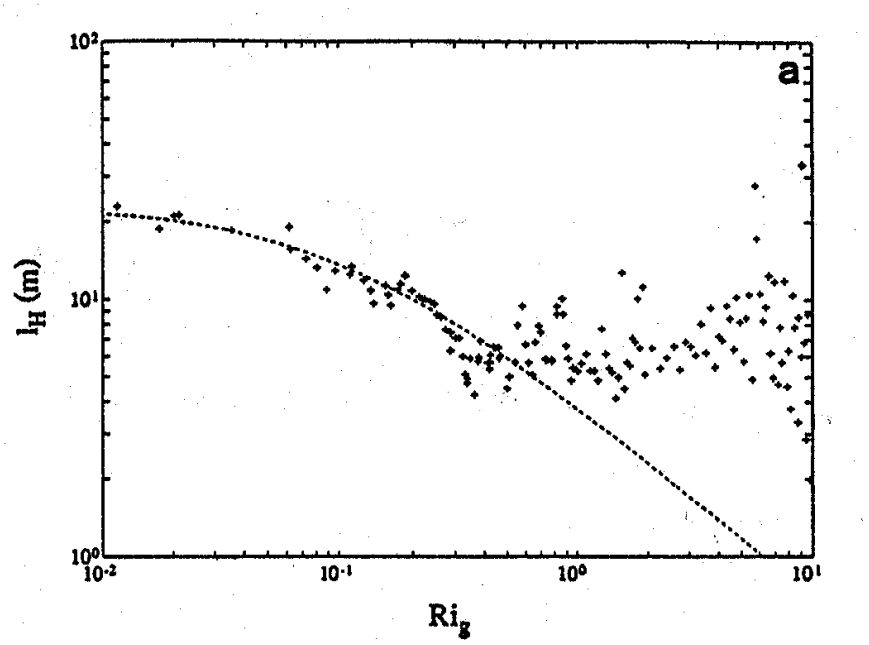

Figure 2. Thermal mixing length against Richardson number. The dashed line is $l_h = l_0[1 + 15Ri_g(1+5Ri_g)^{1/2}]^{-1/2}$, where l_0 is an asymptotic mixing length for the neutral limit, taken to be 23 m. (From Tjernström 1993)

3. Acoustic Sounder Measurement

In addition to thermosondes on micro-thermal balloons, an acoustic sounder can also be used to determine length scales. The acoustic sounder uses acoustic waves scattered by temperature and velocity fluctuations to measure changes in the refractive index of the atmosphere. It transmits an acoustic signal into the atmosphere and detects variations in the thermal structure parameter C_T^2 and the velocity structure parameter C_v^2. For energy backscattered at 180 degrees, the returned signal comes from C_T^2 (Tatarskii 1971). Once C_T^2 is found, equation (9) provides the optical turbulence parameter C_n^2.

a. Acoustic "Radar Equation"

The power returned from the atmosphere was summarized by Neff (1975)

$$\frac{P_r}{E_r} = \left[P_t E_t\right]\left[e^{-2\alpha R}\right]\left[\sigma_0\left(\frac{c\tau}{2}\right)\left(\frac{A}{R^2}G\right)\right], \tag{20}$$

where $\frac{P_r}{E_r}$ is the received power (P_r is the measured electrical power and E_r is the efficiency of conversion from received acoustic power). $P_t E_t$ is the transmitted power (P_t is the electrical power applied to the transducer, E_t is the efficiency of conversion to radiated acoustic power). $e^{-2\alpha R}$ is the round trip loss of power resulting from attenuation by air where α is the average attenuation (m^{-1}) to the scattering volume at range R(m). σ_0 is the backscatter cross section per unit volume and $\frac{c\tau}{2}$ is the maximum effective scattering volume thickness where c is the local speed of sound (ms^{-1}) and τ is the acoustic pulse length (s). $\frac{A}{R^2}G$ is the solid angle subtended by the antenna aperture A (m^2) at range R (m) from the scattering volume, modified by the factor G that accounts for the non-uniform antenna illumination.

Tatarskii (1971) expressed the backscatter cross section σ_0 at 180° as

$$\sigma_0 = \frac{\pi}{2} k^4 \frac{\Phi_T(2k)}{T_0^2}, \tag{21}$$

where $k = 2\pi/\lambda$ is the incident wavenumber, T_0 is the mean temperature, and $\Phi_T(2k)$ is the 3-D spectrum of turbulence. The cross section σ_0 represents the in-phase addition of backscattered waves from temperature inhomogeneities spaced $\lambda/2$ apart along the radial propagation direction. The temperature

inhomogeneities can be represented by the temperature structure parameter C_T^2 Neff (1975) and the volume backscatter cross section for 180° returns becomes

$$\sigma_V = 0.0039 \quad k^{1/3} \frac{C_T^2}{T^2}. \tag{22}$$

The acoustic volume scattering cross section is proportional to the temperature structure parameter and the acoustic wavenumber. This provides the optical structure parameter C_n^2 indirectly with high spatial and temporal resolution.

b. Convective Cells

The heat exchanged between the surface of the earth, the air and the wind shear determine the structure of the boundary layer, the first 1-2 km above the surface. At night radiation into space causes a negative heat flux (heat flux from the atmosphere to the ground) that creates cool dense air next to the surface. This stable air interacts with the wind to create a series of stratified, horizontal layers. During the day, a positive heat flux creates convection cells that rise into the atmosphere with velocities around 5 meters per second. The size of these cells and the vertical thickness of the boundary layer are coupled since convection is the dominant energy source during the day. Under natural conditions, the geometry of these cells is random because of local variations in the surface heat flux and topography. An acoustic sounder detects the ascending portion of the thermal plumes as regions of high turbulence with C_T^2 values around 10^3 times larger that the surrounding air undergoing subsidence. The autocorrelation of C_T^2 or C_n^2 at fixed altitudes as a function of time gives the horizontal separation between the convective cells when multiplied by the wind speed.

Although the vertical thickness of the boundary layer and the lateral size of the convective cells in the atmosphere are related, a functional relationship is not yet known. A measurement of the lateral separation between convective cells is a useful quantity by itself because it determines the horizontal scale of the optical turbulence degradation on ground based optical systems such as laser based air defense weapons.

THIS PAGE INTENTIONALLY LEFT BLANK

II. RESULTS AND DISCUSSION

A. THERMOSONDE DATA

The US Air Force Research Laboratory provided 27 sets of thermosonde data from Vandenberg Air Force Base for analysis: some of the days were cloudy and the probes had either iced up or had high noise levels. In this thesis, only sets of data from the 28 February 2002 launch (2111 LT) and 2 March 2002 (2135 LT) were used. They had high wind speeds of 65 m/s and provided a good opportunity to relate the turbulence and the outer length scales.

Each balloon launch collected two types of data. The first type included variables such as altitude, pressure, temperature, relative humidity and the calculated C_n^2. The data rate was one sample every 1.2 seconds, or about once every 5-6 m of ascent. The second was the GPS derived wind data that included the altitude, wind speed and direction. This data was taken once every 2 seconds, or about once every 8-10 m of ascent. Both data sets included measurements up to 30 km. These variables were used to calculate the thermal outer length scale l_h and the gradient Richardson number Ri_g from equations (17) and (19).

The data collected by the thermosondes were random and needed to be filtered to average the fluctuations and suppress the limited temperature precision. A 5^{th} order Butterworth filter was used to filter the data in both directions to remove the phase distortions. These variables included temperature, pressure and wind velocities.

1. Quantizing Errors in the Temperature Profiles

Figure 3 shows the temperature profiles of the atmosphere for the balloon ascent on 28 February 2002 launch (2111 LT). The resolution of the Vaisala rawinsonde measurements was only 0.1 K. The sudden temperature steps created problems computing vertical temperature gradients. To remove the edge effects of the temperature measurements, the MATLAB FILTFILT function was applied twice to smooth the data. The filter was a 5th order Butterworth filter low pass filter with a normalized cutoff frequency of W_n= 0.2 of the Nyquist sampling frequency. Figure 4 shows a comparison of the filtered and unfiltered temperature profiles with an expanded scale.

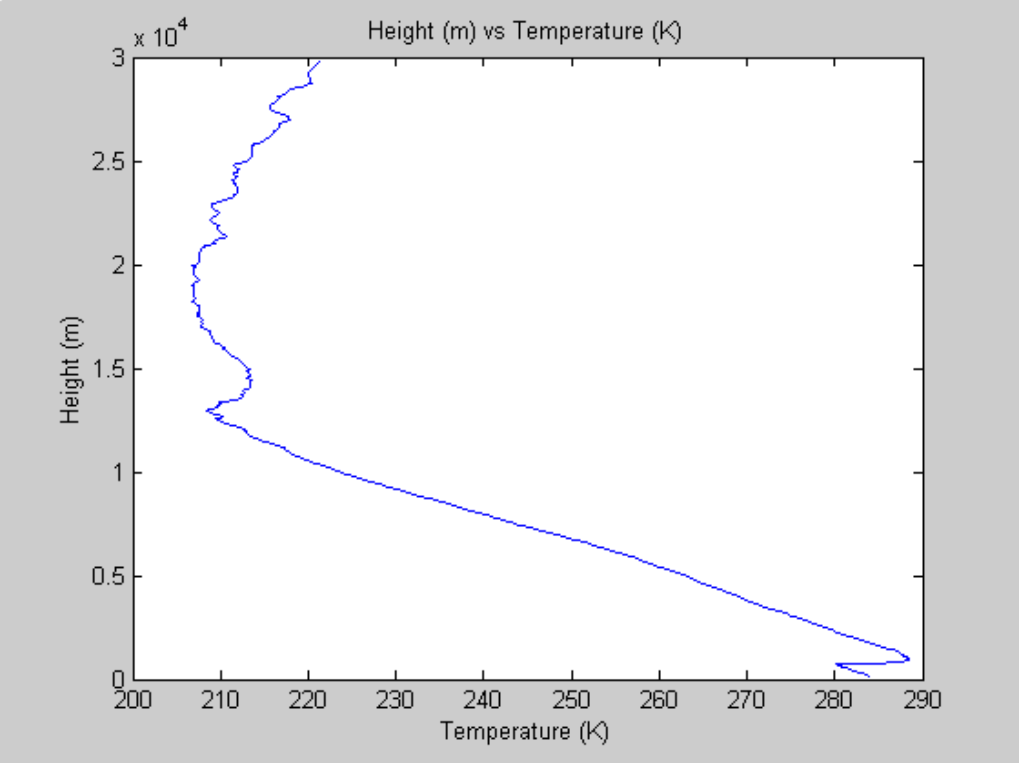

Figure 3. Temperature Profile of Atmosphere (Balloon launched on 28 Feb 02, 2111 LT, Vandenberg Air Force Base)

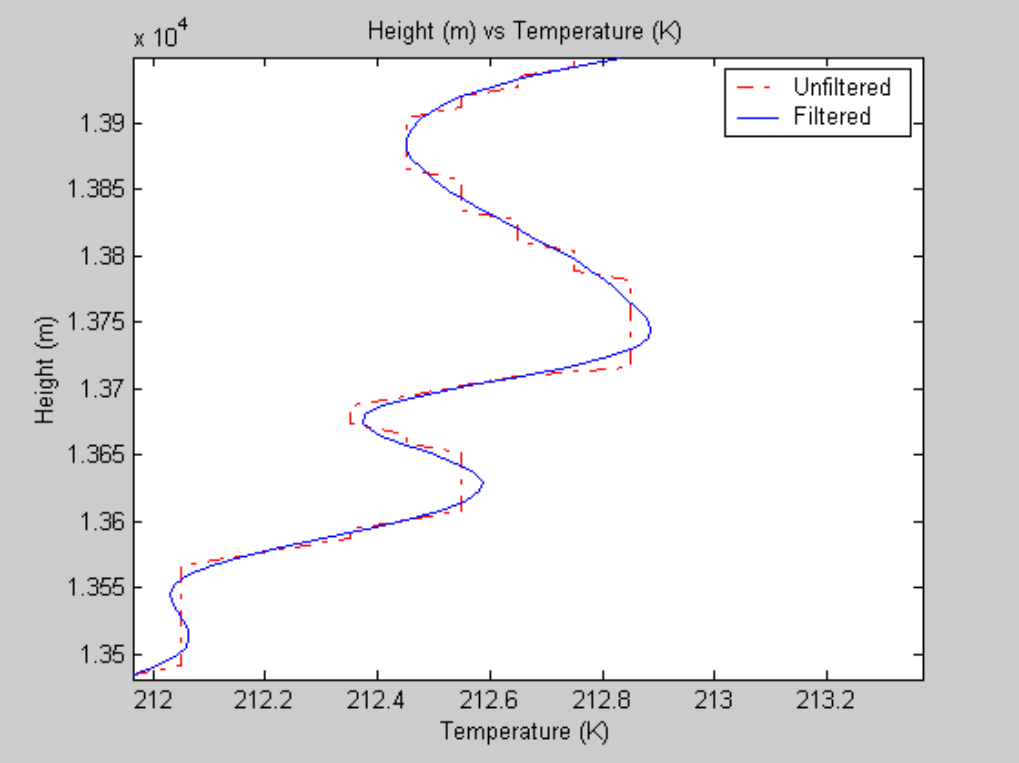

Figure 4. Comparison of Filtered and Unfiltered Temperature Profiles

2. Filtering of Pressure and Altitude

As the balloon ascended into the atmosphere, wind shear perturbations caused the package and the measuring instruments to oscillate like a pendulum. Not only did this swaying motion affect the accuracy of the barometer in determining the pressure, it also biased the altitude calculated from these pressure readings. To overcome this problem a double pass 5^{th} order Butterworth filter with W_n=0.1 removed the swinging from the balloon's pressure measurements. Figures 5 and 6 show the pressure profile and the comparison between filtered and unfiltered pressure readings.

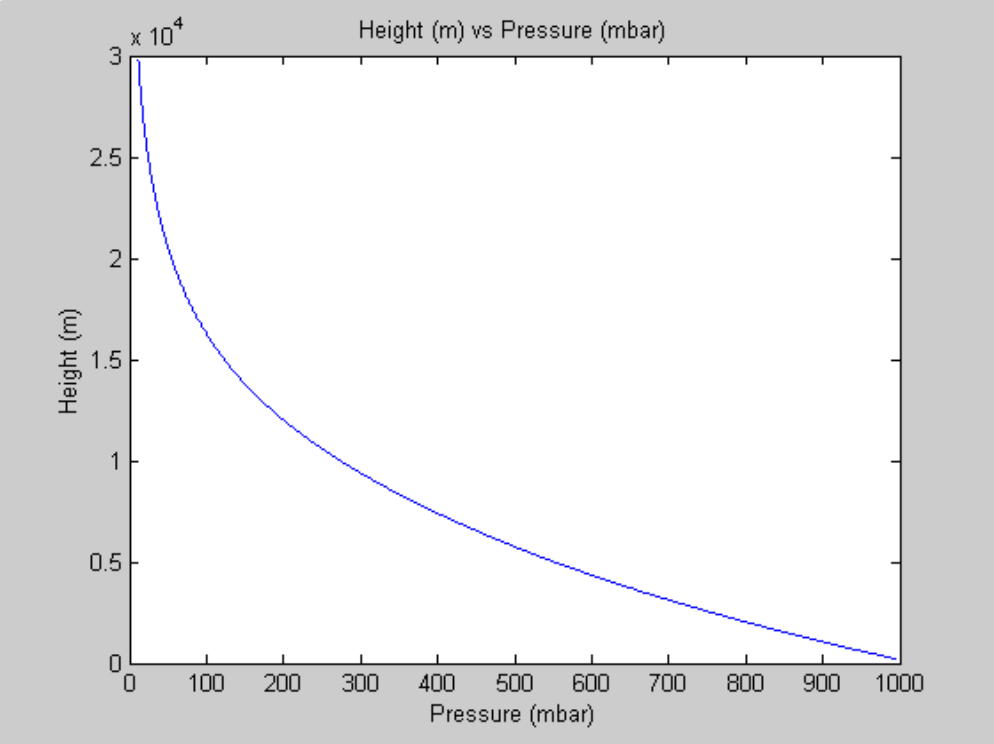

Figure 5. Pressure Profile of Atmosphere (Balloon launched on 28 Feb 02, 2111 LT, Vandenberg Air Force Base)

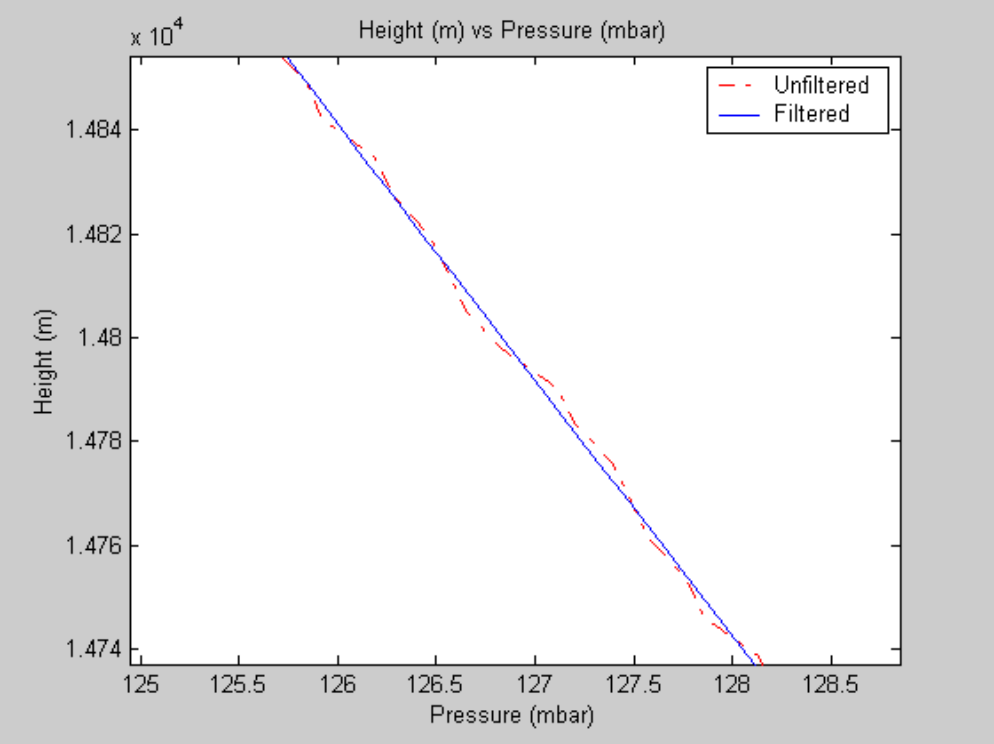

Figure 6. Comparison of Filtered and Unfiltered Pressure Profiles

Pressure is an important variable because it directly affects the calculation of the height of the balloon. To ensure a reliable altitude, the filtered pressure was used to calculate the height of the balloon using the hypsometric equation. Holton (1979) gave the hypsometric equation as:

$$z_2 - z_1 = -\frac{RT_m}{g}\left[\ln\left(\frac{P_2}{P_1}\right)\right], \tag{23}$$

where T_m is the mean temperature between altitudes z_2 and z_1. P_2 and P_1 are the respective pressures at altitudes z_2 and z_1. This calculated hypsometric height gave a more consistent, lower noise representation of the actual ascent as compared to the height readings in the data.

3. Velocity Profile

The GPS wind data were tabulated in terms of magnitude and the direction was expressed in degrees on a 360-degree circle. To compute the gradient Richardson number, the wind data was expressed in two vector components: one component referenced to the east (U wind) and one component referenced to the north (V wind). Since the sampling rate of the turbulence data is higher than the wind data, a cubic spline function in MATLAB interpolated the components of the wind speed to match the time periods of the other meteorological variables. A two pass, 5^{th} order Butterworth filter with a normalized cut-off frequency of W_n=0.3 smoothed the interpolated u and v wind components. The wind profiles are shown in Figure 7 below. Note the strong westerly wind (U wind) at the tropopause.

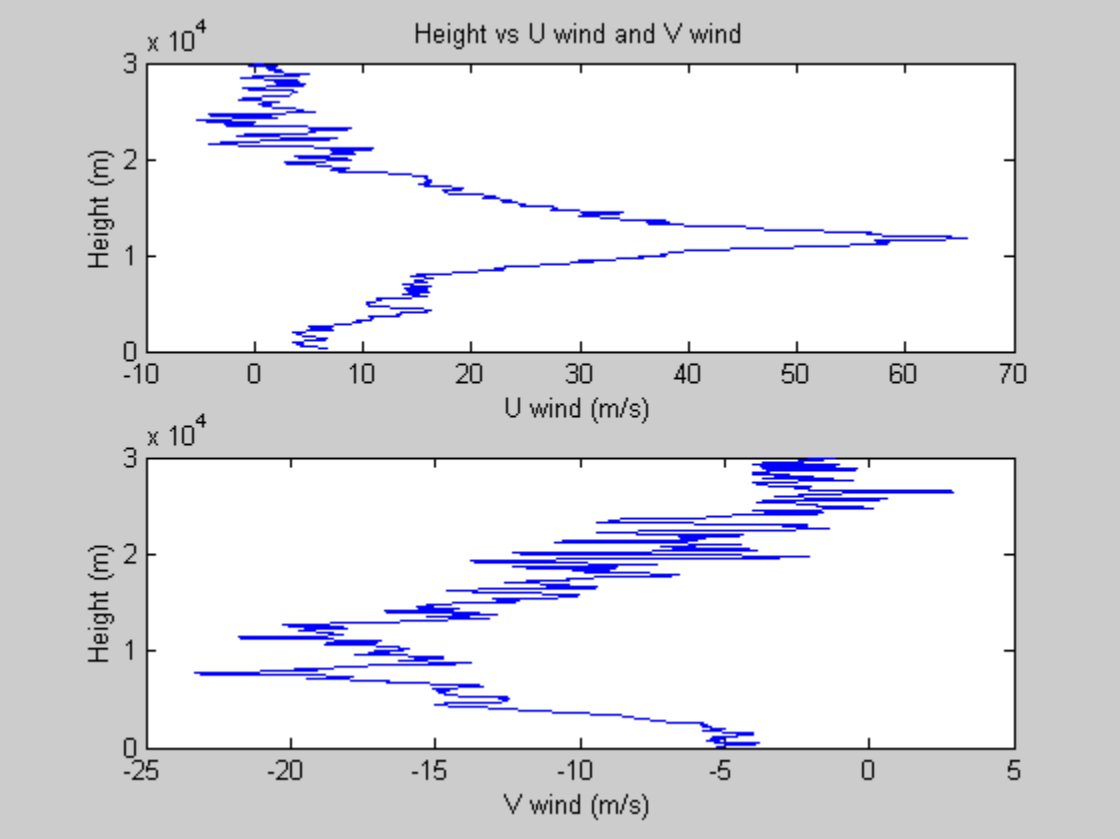

Figure 7. Wind Profiles in the Atmosphere (Balloon launched on 28 Feb 02, 2111 LT, Vandenberg Air Force Base)

4. Potential Temperature

From equation (10), the potential temperature θ depends on the temperature T and the pressure P. Figure 8 shows the potential temperature profile using the filtered temperature and pressure data.

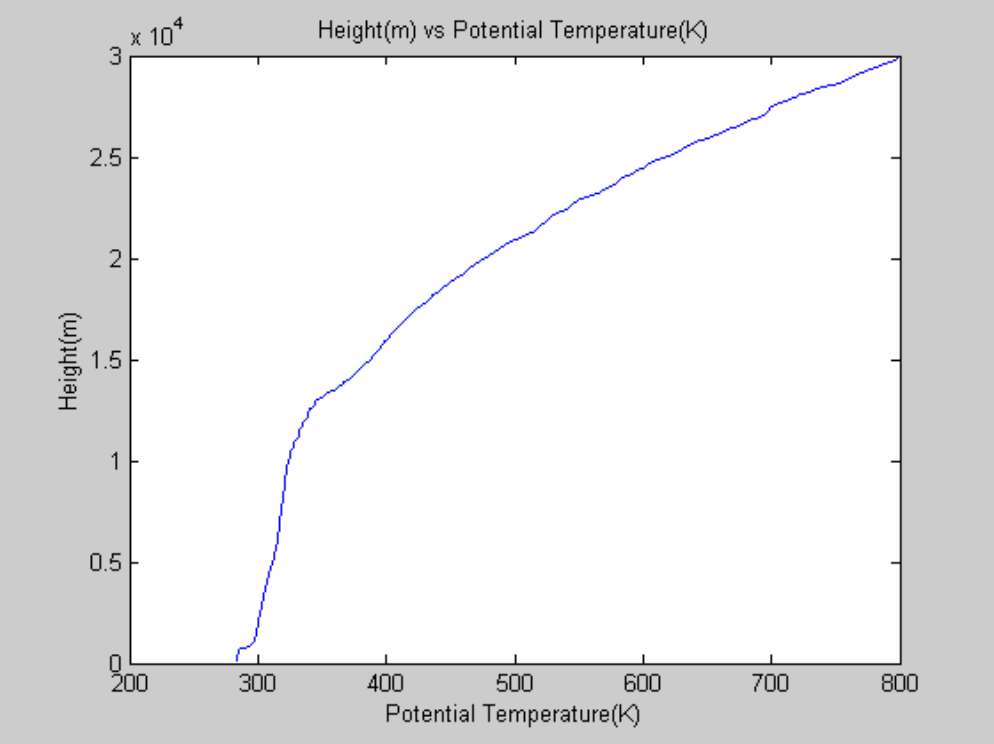

Figure 8. Potential Temperature Profile (Balloon launched on 28 Feb 02, 2111 LT, Vandenberg Air Force Base)

5. Turbulence in the Atmosphere

Figure 9 compares the optical turbulence parameter C_n^2, the potential temperature θ and the gradient Richardson number Ri_g. A neutral region ($\frac{d\theta}{dz} \sim 0$) at 12.8 km is located and it has a corresponding low Richardson number. Similar to the results of Vernin and Avila (1998), this region is the area where there is turbulent mixing of air and it lies between two high C_T^2 or C_n^2 layers. The ~150 m thickness of this neutral region is a measure of the momentum length scale l_m. The thickness of the C_n^2 regions at the upper and lower boundaries of the turbulent region have thermal length scales l_h of 60 and 45 m respectively. The plots show that when atmospheric turbulence is large enough to produce a neutral potential temperature gradient, Ri_g drops to near small values. Correspondingly, two outer length scales l_h form at the boundaries of the neutral

region of the potential temperature. Although the comparison in this case was good, this single case of agreement was not enough to draw a good relationship between the thermal scale length and the gradient Richardson number from the overall data.

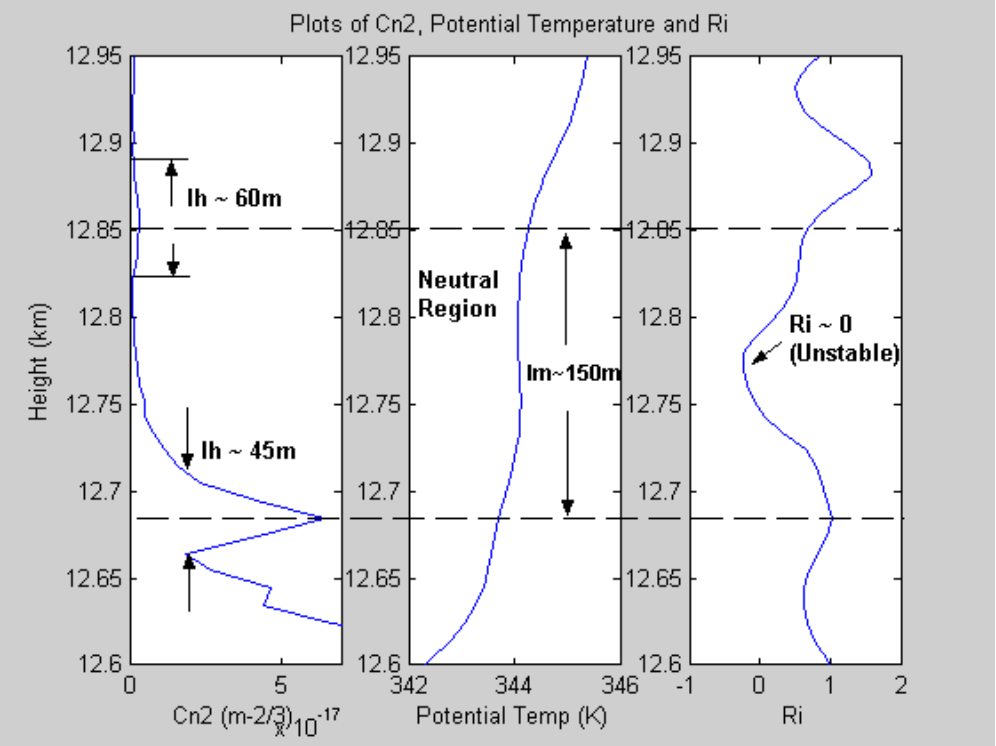

Figure 9. Profiles of optical turbulence parameter C_n^2, the potential temperature θ and the Richardson gradient number Ri_g. (Balloon launched on 28 Feb 02, 2111 LT, Vandenberg Air Force Base)

6. Gradient Richardson Number and Outer Length Scale

The outer length scale l_h and the gradient Richardson number Ri_g were calculated from the turbulence and wind data at every altitude using equations (17) and (19). While there is a single case of agreement between C_n^2, θ and Ri_g at 12.8 km, the data did not reveal a clear relationship between the outer length scale l_h and the Richardson number Ri_g at other heights as shown in Figure 10 below. Figure 11 shows another plot of l_h and Ri_g using data collected on 2 March 2002 launch (2135 LT). The two figures represented different launch

times of the balloon when there were clear skies and minimum noise. Although filtering of the data had been applied, the data scattered over three orders of magnitude, leading to unrealistic outer length scales (l_h > 1000 m) and Richardson numbers (Ri_g > 100). The large scatter made it difficult to determine a functional fit and at best, only an inverse relationship between the outer length scale and the Richardson number is apparent. Part of the scatter may come from using all of the balloon data, regardless of the strength of turbulence.

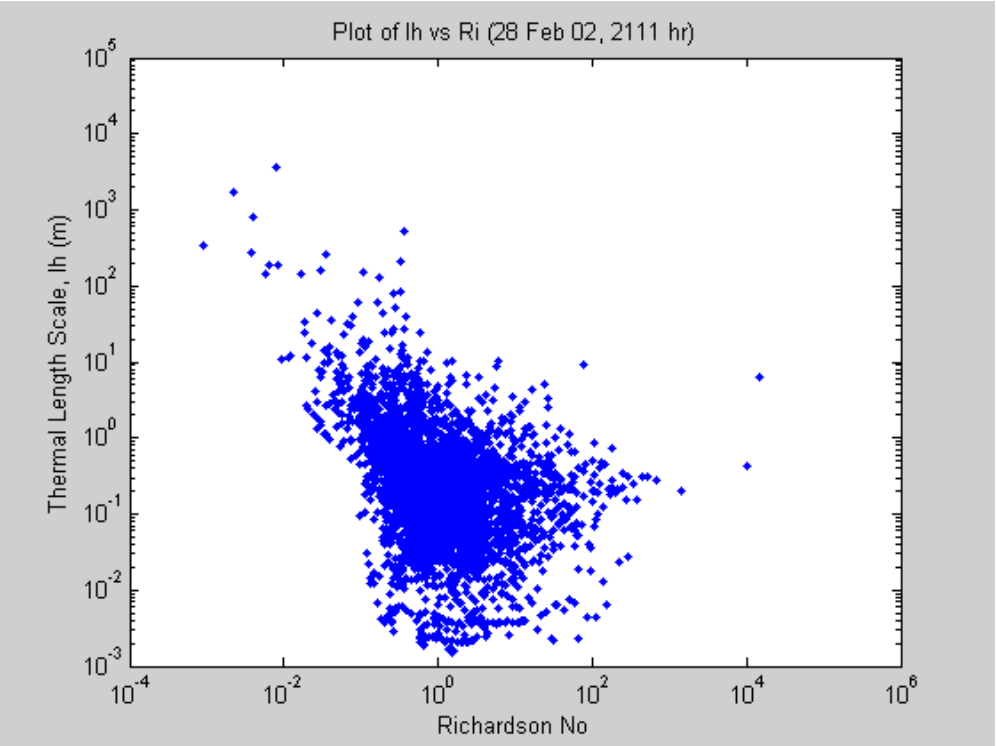

Figure 10. Plot of l_h and Ri_g for every data point in the microthermal balloon data of 28 Feb 02, 2111 LT, Vandenberg Air Force Base.

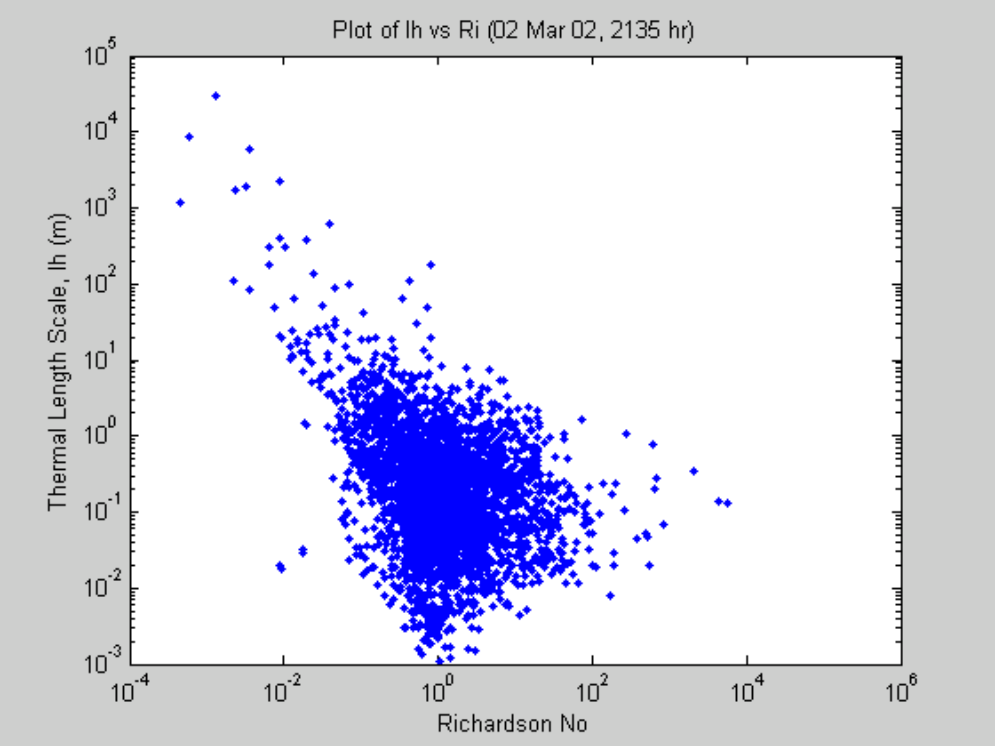

Figure 11. Plot of l_h and Ri_g for every data point in the microthermal balloon data of 2 Mar 02, 2135 LT, Vandenberg Air Force Base

7. Discussion

Although using equation (12) to determine the length scale from the thermal turbulence data was sound, the microthermal and wind data from the balloon launches was not good enough to find a relationship between the thermal length scale and the gradient Richardson number. There were several potential problems that could have resulted in the large scatter of the results shown in Figures 10 and 11. They were (i) swaying of the balloon during ascent, (ii) horizontal inhomogeneity, (iii) under-sampling of the data, or (iv) lack of a meaningful relationship in regions of non-neutral stratification.

The measurement package under the balloon had pendulum-like oscillations by the winds that could not be entirely avoided. The Global Positioning System (GPS) sampled the swaying of the package as a wind component and added noise to the data. Filtering smoothed the data and reduced the effects of the package motion, but also eliminated some of the

vertical resolution needed for computing wind shear. Incorporating fins or other components that introduce drag to the horizontal motion will reduce the swaying of the sonde sensor package; however this would introduce more weight and complexity to the sonde system. This thesis assumed that atmospheric parameters are locally homogenous and since the probes were located less than 1 m apart, horizontal inhomogeneity was unlikely to contribute to the large scatter in the data.

A main source of the large scatter was from under-sampling of the data and from insufficient statistical averaging. Kolmogorov's theory uses ensemble averages to determine turbulence quantities. It is important to have enough temporal or spatial samples to make a meaningful average. Unfortunately, the sample rates of the temperature, pressure and wind data were only once every 1.2 seconds (5-6 m) and 2 seconds (8-10 m), respectively. The C_T^2 thermal sensors and electronics had a bandwidth of about 200 Hz and formed a RMS average sampled every 1.2 seconds. During an ascent, the balloon sensor only makes one pass through a turbulent layer. This snapshot of the atmosphere did not provide the statistical sampling and averaging needed for computing a robust mean value, or a gradient. Redesigning the thermosonde to provide a higher sample rate will help to some extent and this has been done (Walters *et al.* 2001), but the problem of making multiple measurements in a layer to arrive at good mean values still exists. By slowly descending through a layer with an aircraft, Tjernström was able to make an extended sequence of measurements within a single layer, and extract meaningful thermal length scales, although not without great difficulty.

Using all of the microthermal balloon data points created additional problems. Equation (12) should not apply for stable, non-turbulent, atmospheric regions. This would add to the scatter seen in Figures 10 and 11. Attempts to restrict the data set to regions with neutral potential temperature gradients were not successful because of the 0.1K temperature probe resolution, which required filtering, and the long thermal time constant of the temperature probe. These

artifacts obscured the smaller neutral regions and reduced the vertical extent of the larger regions.

B. ACOUSTIC SOUNDER DATA

The acoustic sounder was directed vertically into the atmosphere to collect atmospheric data from 1 March to 29 March 2002 at the Starfire Optical Range in Kirtland Air Force Base, New Mexico. Operating with a 4 KHz, 10-millisecond acoustic pulse, the acoustic sounder sampled the temperature structure parameter C_T^2 between 5 and 100 meters every second. The optical structure parameter C_n^2 was later calculated from the measured C_T^2 values. The Doppler frequencies of the returned signals were also captured. An anemometer located 15m above the ground measured the wind speeds.

In order to measure the convective thermal separation, only the daytime data from 1000-1600 LT were used for analysis. A generally noise free data set collected on 3 March 2002 was chosen to determine the size of the convective cells from the wind and acoustic data before extending the approach to all the data in March 2002.

1. Results

The C_T^2 and Doppler frequencies measured over a 10-minute or 600-second interval (3 March 02 from 1210-1220 hrs) are plotted in Figure 12 below. Figure 12 shows a plot of the magnitude of C_T^2 represented in terms of intensity with the radial Doppler frequencies of $\pm$ 4 m/s as color for a 600 second interval. The red regions are plumes of air (similar to convective cells) moving upwards, and the green regions have zero vertical motion. The region of interest is restricted between 20-50 m because at higher altitudes, extraneous noises tended to corrupt the data.

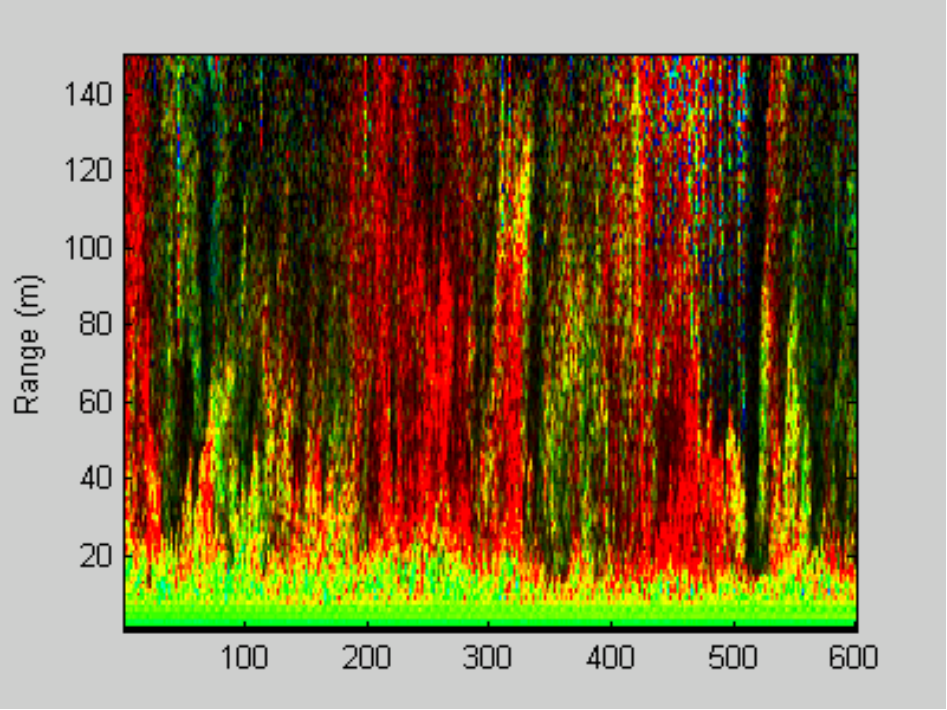

Figure 12. Plot of C_T^2 represented as intensity and vertical velocity as color between 10 and 150 meters over a 600 second interval (3 March 02, from 1210 – 1220 MST). The red regions are plumes of air moving upwards ~4/m/s and the green regions have zero vertical motion.

a. Correlation of Optical Structure Parameter

The volume of atmosphere sampled by the acoustic sounder provided better spatial averaging of C_n^2 than the micro-thermal balloon data. The balloon makes a single transit through a turbulent layer, which is a line through a three dimensional region, whereas the acoustic sounder receives energy from a 4-5 m in diameter, 2 m thick ensonofied volume. To minimize the effects of noise in the data, an average of the C_n^2 values between 20-50 m for individual acoustic pulses formed a 600 second time sequence. The autocorrelation function of this sequence provided the duration between a thermal, convective plume with high C_n^2 values and the adjacent, quiescent region. Multiplying the correlation times by the corresponding anemometer wind speed provided the distance between the regions of C_n^2 minima and maxima.

Figure 13 shows an autocorrelation plot with many maxima and minima that could occur. The complex structure represents small-scale thermal plumes 20 seconds or approximately 200 m across close to the ground in the process of coalescing to form larger thermal cells on the order of 1-2 km. These multiple scales made establishing a size for the thermal plumes subjective, and different processing techniques would give different results. Averages made at 25, 50 and 75 meter altitudes above the ground gave different correlation times, and these times would change depending on the length of the sequence of time 200, 300, 500, 800 seconds used for the autocorrelation. The multiple scales in the data likely reflect the location of the acoustic sounder and the orographic structure of the Starfire Optical Range. The sounder was located near the top, but on the south side of a 70 m hill. The outer scale in convective boundary layers usually scales with the altitude z above the ground, as well as the boundary layer inversion height z_i (Kaimal 1976). The height of the acoustic sounder data above the hill introduces a third scale height that was prevalent in the data of Figure 12 below 40 meters.

A robust technique was needed to determine the size of the thermal cells. The larger scale represented the size of the thermal plumes that form and define the convective boundary layer. A Butterworth filter with a cutoff of W_n = 0.02 of the Nyquist frequency was able to extract the larger scale size consistently. Figure 14 shows the filtered autocorrelation sequence of the data seen in Figure 13. The correlation time was 103 seconds, and the corresponding correlation length was 1.5 km. A stronger 320-second negative correlation appears in Figure 14 at 280-second. This corresponds to a scale of ~4800 meters and the physical source is not yet known.

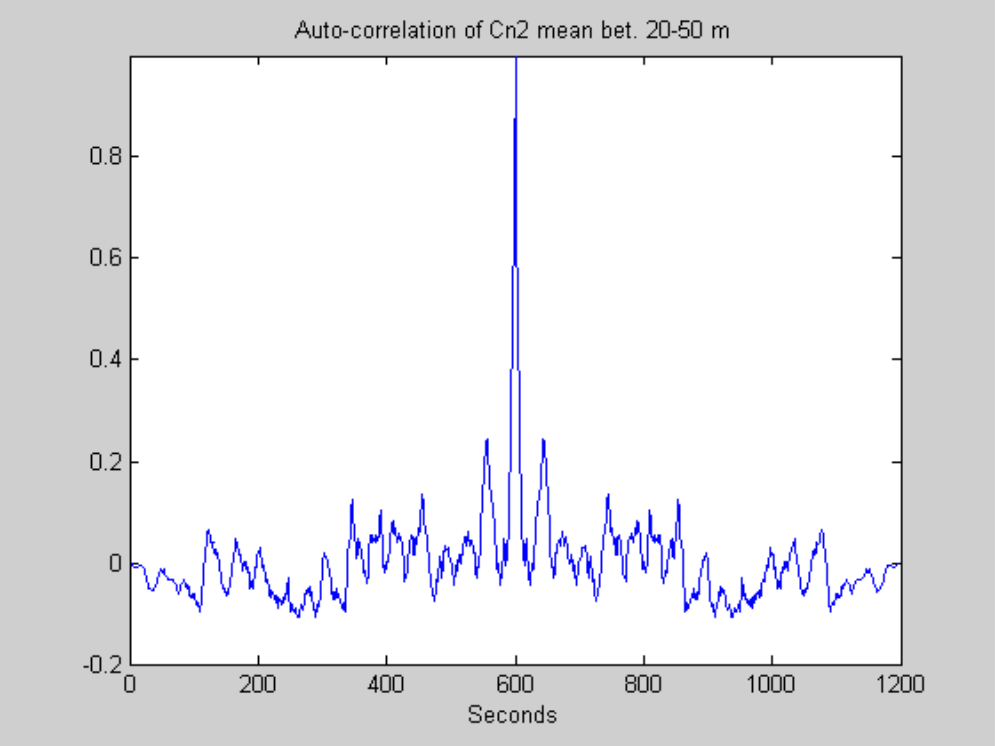

Figure 13. Autocorrelation plot of C_n^2 mean (3 March 02, from 1210 –1220 MST).

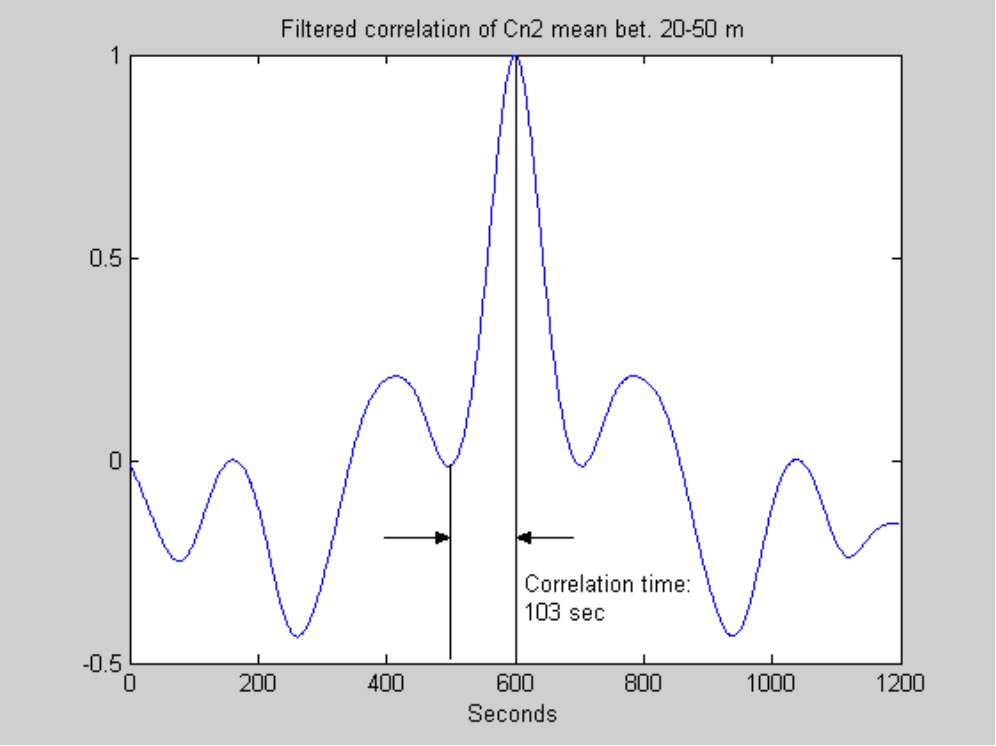

Figure 14. Filtered autocorrelation plot of C_n^2 mean with a 5th order Butterworth filter for both directions with W_n = 0.02.

b. Correlation Length for March 2002

The approach used to establish the autocorrelation time was extended to the acoustic data for the whole month of March 2002, which gave the autocorrelation length by multiplying by the wind velocity. The autocorrelation length was the distance between a vertical column of C_n^2 and the quiescent region adjacent to the column. The histogram of the correlation lengths for March 2002 is shown in Figure 16 below. The mean autocorrelation length was 1590 $\pm$ 770 m.

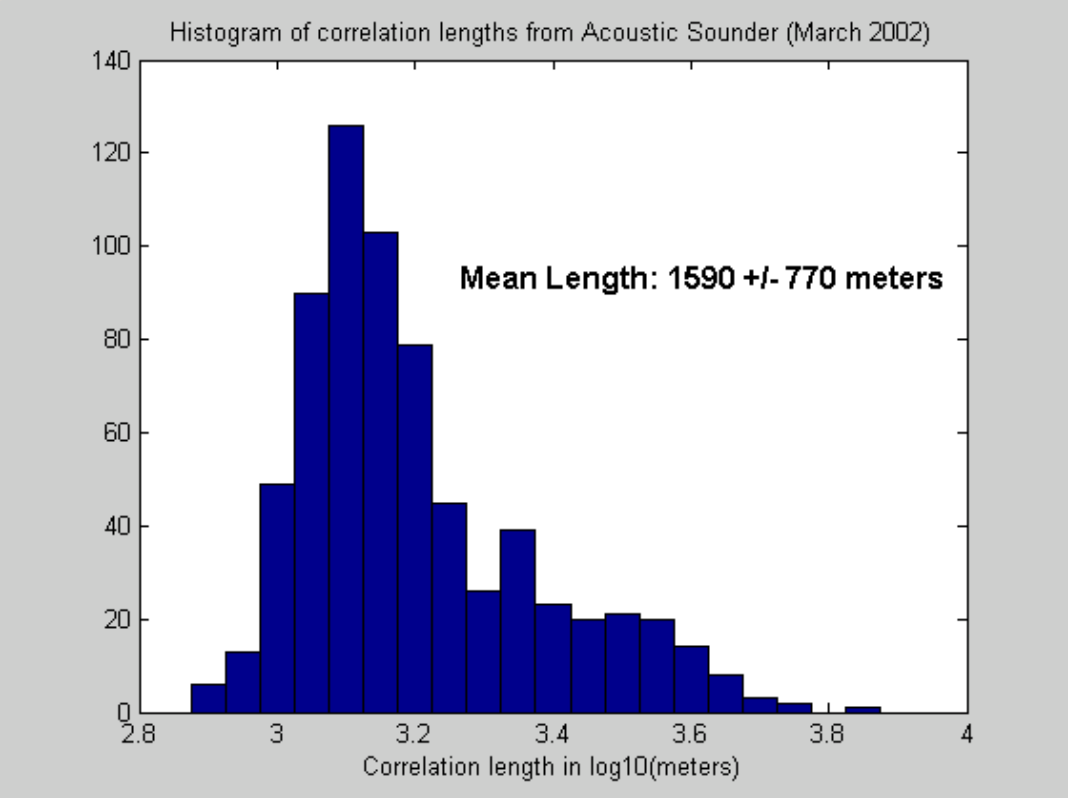

Figure 15. Histogram of midday correlation lengths from acoustic sounder (1000-1600 MST, March 2002).

III. CONCLUSIONS AND RECOMMENDATIONS

A. THERMOSONDE

The results of the investigation showed a large scatter of the thermal outer length scale l_h and the gradient Richardson number Ri_g computed from the micro-thermal balloon data despite filtering the noisy data. Although an inverse relationship between l_h and Ri_g was observed, the large scatter made it difficult to make a meaningful functional fit. Furthermore, the analysis produced unrealistic outer length scales (l_h > 1000 m) and Richardson numbers (Ri_g > 100).

A dominate source of the large scatter was from the under sampling of the turbulence data. The rapid transit of the balloon through a turbulent region caused insufficient statistical sampling to perform meaningful averages of the 20-80 m turbulent layers. In addition, the pendulum swaying of the package required averaging over an oscillation period. This reduced the vertical resolution of the GPS wind data to 50-100 meters, which degraded or removed the subtle wind shears need for accurate Richardson number calculations. Using every data point in the balloon data set may have contributed to the large scatter, since the analysis included non-turbulent regions. An analysis that used only strong turbulent layers might reduce the scatter. Obtaining the thermal length scale l_h or the momentum scale l_m from the balloon data is challenging. Higher temporal resolution will help somewhat, but more robust algorithms are required.

B. ACOUSTIC SOUNDER

The volume backscatter cross-section sampled by the acoustic sounder provided a better sampling of C_T^2 than the micro-thermal balloon. Convective thermal cells appear as regions of strong thermal turbulence to an acoustic sounder. An autocorrelation of a time sequence of C_T^2 at fixed altitudes provided

the size of these convective cells. At least three length scales appeared in the daytime data, associated with the height of the hill above the surrounding area, the height of the data above the hill and the horizontal thermal separation. Strong low pass filtering removed the shorter scale lengths and the mean autocorrelation length between the large thermal cells for the month of March 2002 was 1590 $\pm$ 770 meters. Data from other time periods needs to be analyzed to see how this scale varies throughout the year. The significance of the shorter and larger length scales seen in the autocorrelation analysis needs to be resolved.

LIST OF REFERENCES

Andrén, A. (1990), "Evaluation of a turbulence closure scheme suitable for air-pollution applications," *Journal of Applied Meteorology* (Vol. 29, pp. 224-230).

Andrews, L.C., *et al*. (2001). Theory of optical scintillation: gaussian-beam wave model (p. 273). *Institute Of Physics Publishing Waves In Random Media*. Retrieved November 3, 2003, from http://www.iop.org/EJ/abstract/0959-7174/11/3/306

Beland, R. R. (1996). Propagation through atmospheric optical turbulence, *The infrared & electro-optical systems handbook* (Vol. 2, Chap. 2, pp. 157-232). SPIE Optical Engineering Press.

Brown, J.H., *et al*. (1982). Sonde experiments for comparative measurements of optical turbulence. Instrumentation Papers, No 310, Air Force Geophysics Laboratory, Air Force Systems Command (AFGL-TR-82-0079)

Holton, J. R. (1979) An Introduction to Dynamic Meteorology. (p 19). Second ed. Academic Press, Inc.

Kaimal, J. C., *et al*. (1976). Turbulence structure in the convective boundary layer, *Journal of the Atmospheric Sciences* (Vol. 33, pp. 2152-2169).

Koracin, D. and Rogers, D. P. (1990). Numerical simulations of the response of the marine atmosphere to ocean forcing. *Journal of the Atmospheric Science* (Vol. 43, pp. 592-611).

Max, C. (2003). Lecture 2: Atmospheric turbulence and its effects on image formation. Astronomy 289C - Adaptive Optics. UCSC Department of Astronomy and Astrophysics. Retrieved September 20, 2003, from http://cfao.ucolick.org/~max/289C/Lectures/Lecture%202/Lecture2.v2.pdf

Neff, W. (1975). Quantitative evaluation of acoustic echoes from the planetary boundary layer. NOAA Technical Report. U.S. Department of Commerce, Springfield, VA. U.S. Government Printing Office.

Richardson, D. J. (1997). Solar heating effects on balloon-borne microthermal probes for the airborne laser program, Master's Thesis, Naval Postgraduate School, Monterey, California.

Sasiela R. J. (1994). Electromagnetic Wave Propagation in Turbulence, Evaluation and Application of Mellin Transforms. Springer-Verlag, New York.

Sorbjan, Z. (1989). Structure of the atmospheric boundary layer. (p. 169). Prentice Hall.

Tjernström, M. (1993). Turbulence length scales in stably stratified free shear flow analyzed from slant aircraft profiles. *Journal of Applied Meteorology* (Vol. 32, pp. 948-963).

Tatarskii, V. I. (1961). Wave propagation in a turbulent medium. McGraw-Hill Book Company.

Tatarskii, V. I. (1971). The effects of turbulent atmosphere on wave propagation. NOAA Report No. TT 68-50464, U.S. Department of Commerce, Springfield, VA.

Vernin, J. and Avila, R. (1998). Mechanism of formation of atmospheric turbulence relevant for optical astronomy. An Interstellar Turbulence, J. Franco and A. Carraminana, eds., Cambridge University Press.

Walters, D. L., Chen, C. Y. and Kelly, M. C. (2001). Wavelet analysis of high-resolution temperature data with applications to radio wave scattering. *Radio Science*. (Vol. 36, No. 5, pp 905-926)

INITIAL DISTRIBUTION LIST

1. Defense Technical Information Center
   Ft. Belvoir, VA

2. Dudley Knox Library
   Naval Postgraduate School
   Monterey, CA

3. Donald L. Walters
   Code PH/WE
   U.S. Naval Postgraduate School
   Monterey, CA

4. Douglas K. Miller
   Code MR/DM
   U.S. Naval Postgraduate School
   Monterey, CA

5. James H. Luscomb
   Code PH/LJ
   U.S. Naval Postgraduate School
   Monterey, CA

6. Professor Yeo Tat Soon
   Director, Temasek Defence Systems Institute
   National University of Singapore